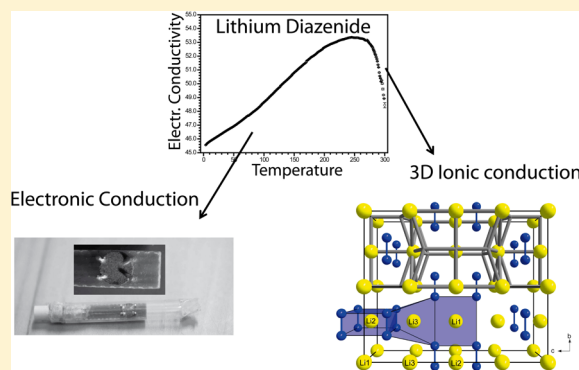


Electronic and Ionic Conductivity in Alkaline Earth Diazenides  $M_{AE}N_2$  ( $M_{AE} = Ca, Sr, Ba$ ) and in  $Li_2N_2$ Sebastian B. Schneider,<sup>†</sup> Martin Mangstl,<sup>†,‡</sup> Gina M. Friederichs,<sup>†</sup> Rainer Frankovsky,<sup>†</sup> Jörn Schmedt auf der Günne,<sup>†,‡</sup> and Wolfgang Schnick<sup>\*†</sup><sup>†</sup>Department of Chemistry, University of Munich (LMU), Butenandtstr. 5-13, D-81377 Munich, Germany<sup>‡</sup>Department of Chemistry, University of Siegen, Adolf-Reichwein-Straße, 57068 Siegen, Germany

## Supporting Information

**ABSTRACT:** Electrical conductivity measurements of alkaline earth diazenides  $SrN_2$  and  $BaN_2$  revealed temperature-dependent metal-like behavior. As  $CaN_2$  is isotypic with  $SrN_2$  its electronic properties are supposed to show similar characteristics. For the alkali diazenide  $Li_2N_2$ , the corresponding measurement shows not only the typical characteristics of metallic materials but also an unexpected rise in electrical conductivity above 250 K, which is consistent with an ionic contribution. This interpretation is further corroborated by static  $^6Li$  and  $^7Li$  nuclear magnetic resonance measurements (NMR) of the spin-lattice relaxation time ( $T_1$ ) over an extended temperature range from 50 to 425 K. We observe a constant Heitler-Teller product ( $T_1T$ ) as expected for metals at low temperatures and a maximum in the temperature-dependent relaxation rates, which reflects the suggested ionic conductivity. A topological structural analysis indicates possible 3D ion migration pathways between two of the three crystallographic independent Li positions. A crude estimate of temperature-dependent self-diffusion coefficients  $D(T)$  of the lithium motion classifies  $Li_2N_2$  as a mixed electronic/ionic conductor.

**KEYWORDS:** diazenide, electrical conductivity, lithium ion conduction, nuclear magnetic resonance (NMR), self-diffusion coefficient



## INTRODUCTION

Due to numerous applications of binary metal-nitrogen compounds, their synthesis and characterization had and still has a remarkable impact on solid-state and materials chemistry.<sup>1–9</sup> Besides the long known nitrides and azides with  $N^{3-}$  and  $[N_3]^-$  anions, respectively, a third class of nitrogen based anions proved their existence only very recently, the latter consisting of homonuclear dinitrogen units, namely  $[N_2]^{x-}$  ( $x = 1–4$ ).<sup>10–33</sup> Besides the paramagnetic dinitrogen anions  $[N_2]^-$  and  $[N_2]^{3-}$ , which so far have only been observed in molecular complexes,<sup>10–16</sup> it was  $[N_2]^{2-}$  and  $[N_2]^{4-}$  ions that could have been synthesized in solid-state compounds.<sup>17–33</sup> The 14 electron ion  $[N_2]^{4-}$  is isosteric with peroxide  $[O_2]^{2-}$  and thus was named pernitride,<sup>24–33</sup> whereas  $[N_2]^{2-}$ , representing a deprotonated diazene  $N_2H_2$  with a  $N=N$  double bond has been denominated diazenide.<sup>17–23</sup>

The first binary representatives containing  $[N_2]^{2-}$  anions were  $SrN_2$  and  $BaN_2$ , which have been synthesized under nitrogen pressure in a specialized autoclave system.<sup>17–21</sup> In order to further extend this class of metal diazenides, we recently have targeted new synthetic approaches and were successful employing controlled thermal decomposition of ionic azides in a multianvil device under high-pressure/high-temperature (HP/HT) conditions.<sup>22,23</sup> Besides the two known

diazenides, we obtained and characterized novel  $CaN_2$  and the first alkali diazenide, namely  $Li_2N_2$ .<sup>22,23</sup>

With a high difference in electronegativity between cations and anions, these diazenide compounds suggest rather ionic behavior, although having a black metallic luster. In addition, corresponding theoretical calculations on their electronic structure revealed that these compounds should exhibit metallic characteristics.<sup>18,22,23,34</sup> This is somehow surprising, as simple compounds containing corresponding homonuclear anions made up of elements on either side of the element nitrogen in the PSE, namely acetylenide  $[C_2]^{2-}$  or peroxide compounds, clearly show ionic and thus insulating or at least semiconductive behavior.<sup>35–37</sup> In addition, stretching vibrations of the double-bonded dinitrogen anions were observed in FTIR measurements of the mentioned diazenides as distinct features at about  $1325–1375\text{ cm}^{-1}$  (see Figure S1 in the Supporting Information, SI).<sup>22,23</sup> In fact, applying the correlation method<sup>38</sup> for allowed vibrations of the diazenide ions in the corresponding crystal structures, we were successful by predicting infrared-active modes for all of these diazenides.<sup>22,23</sup>

Received: April 11, 2013

Revised: September 11, 2013

Published: October 1, 2013

This observation rather contradicts metal-like behavior as for metallic compounds infrared-active features at such high energies usually do not occur. Additional theoretical considerations on the existence of hitherto unknown diazenide compounds revealed that  $\text{FeN}_2$ ,  $\text{ZnN}_2$  and  $\text{LaN}_2$  should be thermodynamically stable at ambient conditions and exhibit again metallicity.<sup>33,39,40</sup> However, the true character of an either metallic or ionic formulation of diazenides based on experimental data still leaks evidence.

In the case of  $\text{Li}_2\text{N}_2$ , potential lithium ionic conduction is, however, thought to interfere with assumed metallic, electronic conductivity. As the interest in and demand for  $\text{Li}^+$  ion conductors still increase due to their industrial applications such as solid-state batteries,<sup>41–43</sup> it is important to fully characterize  $\text{Li}_2\text{N}_2$ . In order to investigate a potential ionic conduction, lithium nuclear magnetic resonance (NMR) is a suitable tool.<sup>44–46</sup> As it already has been shown for  $\text{Li}_3\text{N}$  and various  $\text{Li}^+$  containing compounds,<sup>47–53</sup> it is possible to estimate activation energies  $E_A$  and diffusion coefficients  $D(T)$  for the lithium migration from temperature-dependent  $^6\text{Li}$  and  $^7\text{Li}$  spin-lattice relaxation (SLR) experiments.

In the present work, we report on an experimental study of unsettled metal-like behavior in diazenide compounds. Conductivity measurements between 3.5 and 300 K are presented and measured specific conductivities are classified and discussed with respect to those of metals, semiconductors and insulators. Ionic and electronic contributions to the electrical conductivity in  $\text{Li}_2\text{N}_2$  were further investigated from temperature-dependent  $^6\text{Li}$  and  $^7\text{Li}$  NMR. The results obtained with different experimental techniques combined with a topological analysis of lithium migration pathways allow us to estimate a activation energy  $E_A$ , the dimensionality and temperature-dependent self-diffusion coefficients  $D(T)$  of the lithium motion.

## ■ EXPERIMENTAL SECTION

**Synthesis of Azides.** Nondoped  $\text{LiN}_3$  was obtained by precipitation from its aqueous solution (Sigma-Aldrich, 20 wt % solution in water) by evaporation in vacuum, whereas  $^6\text{LiN}_3$  was precipitated in diethylether by addition of excess  $\text{NaN}_3$  (Acros Organics, 99%) to a suspension of  $^6\text{LiCl}$  (Sigma-Aldrich, 95 atom %  $^6\text{Li}$ , 99%) in absolute ethanol, as described in literature.<sup>54–56</sup> Strontium and barium azide are obtained by the reaction of the corresponding hydroxides (Sigma-Aldrich, 99.995%) with an aqueous solution of  $\text{HN}_3$ , as reported in the literature.<sup>54,55</sup> The extremely dangerous  $\text{HN}_3$  is distilled from  $\text{NaN}_3$  (Acros Organics, Geel, Belgium, 99%) and  $\text{H}_2\text{SO}_4$ . The solid azides are dried over  $\text{P}_4\text{O}_{10}$  using a vacuum desiccator (24 h). A general procedure for the synthesis of the azides of the heavier alkaline earth metals is described in the literature.<sup>56</sup>

**Caution!** Due to the very low thermal and mechanical shock resistance of  $\text{HN}_3$ , only very small quantities should be used. Therefore, whenever working with  $\text{HN}_3$ , efficient protective clothing such as face protection, a leather coat, and steel reinforced gloves must be worn.

**Synthesis of Diazenides.**  $^6\text{Li}_2\text{N}_2$ , nondoped  $\text{Li}_2\text{N}_2$ ,  $\text{SrN}_2$  and  $\text{BaN}_2$  were synthesized at distinct HP/HT-conditions in a modified Walker-type module in combination with a 1000 t press (both devices from the company Voggenreiter, Mainleus, Germany), according to literature.<sup>22,23</sup> The as-obtained azide was carefully ground, filled into a cylindrical copper ( $\text{Li}_2\text{N}_2$ ) or boron nitride ( $\text{M}_{\text{AE}}\text{N}_2$ ) crucible (Henze BNP GmbH, Kempten, Germany) and sealed with a fitting boron nitride plate. As pressure medium, precastable  $\text{MgO}$ -octahedra (Ceramic Substrates & Components, Isle of Wight, U.K.) with edge lengths of 18 mm (18/11 assembly) were applied. Eight tungsten

carbide cubes (Hawedia, Marklkofen, Germany) with truncation edge lengths of 11 mm compressed the octahedra. Details of the setup can be found in the literature.<sup>57–61</sup>  $\text{Li}_2\text{N}_2$  ( $\text{SrN}_2$ ,  $\text{BaN}_2$ ) was synthesized in a 18/11 (18/11, 18/11) assembly, which was compressed up to 9 (9, 3) GPa at room temperature within 217 (214, 68) minutes, then heated up to 750 (850, 750) K in 10 (30, 30) minutes, kept at this temperature for 50 (15, 15) minutes and cooled to room temperature in 10 (10, 10) minutes. Subsequently, pressure was released over a period of 633 (623, 183) minutes. The recovered  $\text{MgO}$ -octahedron was broken apart under inert conditions in a glovebox (Unilab, MBraun, Garching;  $\text{O}_2 < 1$  ppm,  $\text{H}_2\text{O} < 1$  ppm), and the sample was carefully isolated from the surrounding boron nitride crucible. A black metallic powder of the corresponding diazenide is obtained, extremely sensitive to moisture. Each diazenide was analyzed by means of powder X-ray diffraction patterns, which were recorded with a STOE Stadi P powder diffractometer (STOE, Germany) in Debye–Scherrer geometry using  $\text{Ge}(111)$  monochromated Mo- and  $\text{Cu K}\alpha_1$ -radiation, respectively (0.7093 Å and 1.54056 Å).

$\text{Li}_2\text{N}_2$  crystallizes in space group *Immm* (no. 71) with  $a = 3.1181(4)$ ,  $b = 4.4372(4)$ ,  $c = 10.7912(16)$  Å,  $V = 149.31(3)$  Å<sup>3</sup>, and  $Z = 4$ ; Li1 in (2a), Li2 in (2c), Li3 in (4i) with  $z = 0.2510(6)$ , and N1 in (8l) with  $y = 0.1466(5)$  and  $z = 0.62321(19)$ .<sup>22</sup>  $\text{SrN}_2$  crystallizes in a tetragonally distorted NaCl-type structure in space group *I4/mmm* (no. 139) with  $a = 3.8054(2)$  Å,  $c = 6.8961(4)$  Å,  $V = 91.17(1)$  Å<sup>3</sup> and  $Z = 2$ ; Sr1 in (2a) and N1 in (4e) with  $z = 0.4016(4)$ .<sup>23</sup> The crystal structure of  $\text{BaN}_2$  is of monoclinic symmetry (*C2/c* no. 15) with  $a = 7.1608(4)$  Å,  $b = 4.3776(3)$  Å,  $c = 7.2188(4)$  Å,  $\beta = 104.9679(33)^\circ$ ,  $V = 218.61(2)$  Å<sup>3</sup>, and  $Z = 4$ ; Ba1 in (4e) with  $y = 0.2006(2)$  and N1 in (8f) with  $x = 0.3023(18)$ ,  $y = 0.1547(39)$ , and  $z = 0.0508(19)$ .<sup>23</sup> The crystallographic data of the corresponding diazenides are taken from the literature.<sup>22,23</sup>

**Conductivity Measurements.** For the measurements of  $\text{SrN}_2$  and  $\text{BaN}_2$ , two reaction batches of each diazenide were combined, whereas for the measurement of  $\text{Li}_2\text{N}_2$  an overall of eight batches had to be merged due to the small sample amount obtained upon synthesis. In addition, each product of a HP/HT-synthesis was analyzed separately by means of powder X-ray diffraction to rely on a successful synthesis of the corresponding diazenide.

The electrical measurements were performed with a self-built susceptometer consisting of a Janis shi-950 two-stage closed-cycle Cryostat with  $^4\text{He}$  exchange gas (Janis Research Company, Wilmington, U.S.A.) and a dual-channel temperature controller (model 332 by LakeShore, Westerville, U.S.A.). A Keithley Source-Meter 2400 (Cleveland, U.S.A.) was available as current source, which was used to create square waves with amplitudes of 2  $\mu\text{A}$  to 5 mA and frequencies of either 2 or 0.4 Hz (1 or 5 PLC, respectively). The differential voltage drop between signal-high and signal-low was recorded with a Keithley 2182 Nano-Voltmeter and used to calculate the sample resistance in one direction according to Ohm's law and the specific resistance according to the Van-der-Pauw approximation.<sup>62</sup>

For the measurements cold pressed (10 kN) pellets of nonsintered diazenides (diameter, 4.0 mm; thickness, 0.5–0.9 mm) were produced. Applying the four-probe method, the pellet was contacted with four equidistant probes using silver conducting paint. As the diazenides were extremely sensitive to moisture, all preparations had to be done under inert atmosphere in a glovebox. A current of  $0.15\text{--}0.3 \cdot 10^{-3}$  A was applied and the potential difference was measured as a function of the temperature upon cooling and heating (300 to 3.5 K) yielding the specific conductivity. No superconductivity was observed.

**$^6\text{Li}$  and  $^7\text{Li}$  solid-State Nuclear Magnetic Resonance.** The static  $^7\text{Li}$  and  $^6\text{Li}$  NMR spectra were recorded with a Bruker Avance III NMR spectrometer at a frequency of 194.37 and 73.60 MHz, respectively, which corresponds to an external magnetic field of 11.7 T. For temperature-dependent measurements, the spectrometer was equipped with different commercial static variable-temperature probes. For temperatures above approximately 160 K a double-resonance SOL5 probe from Bruker Biospin was used, for temperatures below 160 K a probe from the same company was used which consists of a He continuous flow cryostat (model STVP-XG, Janis Research Company, Wilmington, MA, U.S.A.) and a single channel probe

with two CERNOX temperature sensors and self-made coils. The sample was inserted into the coils made of manganin wire for the low-temperature  ${}^7\text{Li}$  experiments and silver plated copper wire in case of the  ${}^6\text{Li}$  experiments. The sample was sealed in an airtight glass tube under vacuum.  $T_1$  spin-relaxation times were measured with a saturation recovery experiment. The one-dimensional  ${}^7\text{Li}$  static NMR spectra were acquired with a  $\pi/2$  pulse length of 1.5  $\mu\text{s}$  and a recycle delay minimum three times larger than  $T_1$ . The solid-echo  ${}^6\text{Li}$  static NMR spectra were acquired with a  $\pi/2$  pulse length of 1.31  $\mu\text{s}$  and a recycle delay minimum three times larger than  $T_1$ .<sup>63</sup>

## RESULTS AND DISCUSSION

**Conductivity Measurements.** For metals, resistance is temperature-dependent and supposed to decrease with decreasing temperature. The resistance of a semiconductor decreases with increasing temperature and shows an abrupt decay, once the electrons can be excited from the valence band into the conductive band. Insulators only become conductive at very high temperatures and show exceptional high specific resistances at ambient temperature. Taking these classifications into account and comparing them to the observed conductivity curve of the diazenides, the ambiguity whether there is metallicity in diazenides or not can now be referenced.

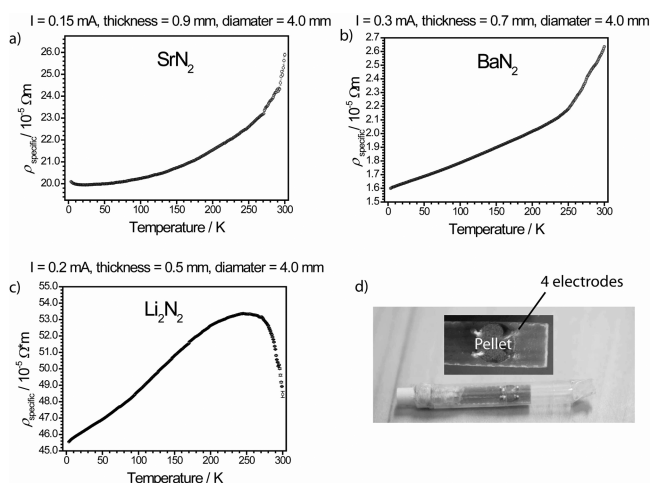


**Figure 1.** Specific resistance for  $\text{SrN}_2$  (a),  $\text{BaN}_2$  (b), and  $\text{Li}_2\text{N}_2$  (c) with temperature; experimental setup for the measurements illustrating the pellet placed between four electrodes (d).

Figure 1, parts a, b, and c, show the specific resistance curves for  $\text{SrN}_2$ ,  $\text{BaN}_2$ , and  $\text{Li}_2\text{N}_2$ , respectively, obtained upon cooling the prefabricated pellets. Figure 1d depicts the pellet of black

colored  $\text{Li}_2\text{N}_2$  mounted onto the sample holder for conductivity measurements.

$\text{SrN}_2$  and  $\text{BaN}_2$  show a decrease of specific resistance with decreasing temperature, typical for metals. However, it has to be stated that the pellets have not been sintered before the measurements but were only cold pressed to avoid any oxidation of these highly moisture-sensitive compounds.<sup>64</sup>

For  $\text{Li}_2\text{N}_2$ , the specific resistance increases up to a maximum temperature of about 250 K and finally decreases with a further decrease of temperature as expected for metals. Thus, true metal-like behavior is only observed at temperatures below 250 K. The change in conductivity from 250 K to higher temperatures needs a different explanation, for example  $\text{Li}^+$  ion conductivity, thermal activation across a band gap (intrinsic doping), or a phase transition. However, the latter explanation of unexpected resistivity in  $\text{Li}_2\text{N}_2$  can be excluded as previous temperature-dependent *in situ* powder X-ray diffraction already revealed no phase transition below ambient conditions.<sup>22</sup> Interestingly, it is only the  $\text{Li}^+$  ion containing diazenide showing such a distinct feature in its specific resistance.

Table 1 lists the obtained resistivity values for  $\text{SrN}_2$ ,  $\text{BaN}_2$  and some selected elements<sup>65,66</sup> at ambient temperature (300 K) and for  $\text{Li}_2\text{N}_2$  at 250 K.

Obviously, the specific values of the diazenides are intermediate to those of pure metals and semiconductors. However, as the pellets have not been sintered for the measurements, they definitively do contain a large number of grain boundaries inhibiting perfect conductivity properties. In addition, the products upon HP/HT-synthesis still show oxide impurities in case of the alkaline earth diazenides and an unknown minor side phase with  $\text{Li}_2\text{N}_2$ .<sup>22,23</sup> Taking all these facts into account, the true values of resistivity are thought to match better with pure metals. Thus, it is the curve progression indicating true metal-like behavior for all diazenides.

### ${}^6\text{Li}$ and ${}^7\text{Li}$ Solid-State Nuclear Magnetic Resonance.

In order to investigate the hypothesis of a beginning  $\text{Li}^+$  ion conduction at elevated temperatures being responsible for the unexpected change in resistivity with temperature, variable temperature measurements of the spin-lattice relaxation (SLR) times ( $T_1$ ) of  ${}^6\text{Li}$  and  ${}^7\text{Li}$  nuclei were performed from 170 to 390 K and from 50 to 425 K, respectively. In the following, we will first discuss the low-temperature regime which, consistently with the macroscopic electrical conductivity measurements, gives evidence of the metallic character of  $\text{Li}_2\text{N}_2$ . Then, we will discuss the observed anomaly at increased temperatures reaching up to the decomposition point at about 385 K (depending on synthesis conditions).<sup>67</sup>

**Table 1.** Specific Resistance of Diazenides ( $\text{SrN}_2$  and  $\text{BaN}_2$  at Ambient Temperature;  $\text{Li}_2\text{N}_2$  at 250 K) and Selected Elements<sup>65,66</sup> As Well As Their Corresponding Color and Resulting Electronic Behavior

compd.	$\rho_{\text{specific}} [\Omega\text{m}]$	color	characteristics
$\text{Li}_2\text{N}_2$	$5.33 \cdot 10^{-4}$	black	this work
$\text{SrN}_2$	$2.32 \cdot 10^{-4}$	black-bronze	this work
$\text{BaN}_2$	$0.23 \cdot 10^{-4}$	black-bronze	this work
$\text{Fe}^{65}$	$1.0 \cdot 10^{-7}$	gray-metallic	metallic
$\text{Pb}^{65}$	$2.2 \cdot 10^{-7}$	gray-metallic	metallic
$\text{Mn}^{66}$	$1.43 \cdot 10^{-6}$	steelwhite-metallic	metallic
amorphous carbon <sup>66</sup>	$\sim 6 \cdot 10^{-5}$	black	semiconductive
$\text{Te}^{66}$	$\sim 3 \cdot 10^{-3}$	silverwhite-metallic	semiconductive
diamond <sup>65</sup>	$> 0.1 \cdot 10^9$	transparent	insulating

Metals at low temperatures have a characteristic relaxation behavior due to the unpaired electrons close to the Fermi level which leads to a constant Heitler-Teller product  $T_1T$ .<sup>68–70</sup> Often this is accompanied by a drastic change of the chemical shift. The difference in chemical shift to diamagnetic materials is termed Knight shift  $K$  and often specified in % because of its enormous size in some cases. In case of metallic Li, the Knight shift  $K$  is small and only of the order of 400 ppm. Even with modern quantum chemical methods, it is difficult to predict the Knight shift. Korringa<sup>69,71</sup> derived a formula that relates the Knight shift  $K$  to the Heitler-Teller product  $T_1T$  (see eq 1) given the conduction electrons form a free electron gas, where  $\gamma_e$  and  $\gamma_n$  refer to the electron and nuclear gyromagnetic ratios, respectively.

$$T_1T = \frac{h}{8\pi^2k_BK^2} \frac{\gamma_e^2}{\gamma_n^2} \quad (1)$$

In the case of  $\text{Li}_2\text{N}_2$ , we obtained temperature SLR time constants both for  $^6\text{Li}$  and for  $^7\text{Li}$  ( $^7\text{Li}$ , Figure 2;  $^6\text{Li}$ , SI Figure S2). As expected, we observe constant Heitler-Teller products  $T_1T$  in the low-temperature region. The Korringa formula (see eq 1) predicts a quotient of the Heitler-Teller products

$$\frac{T_1T(^7\text{Li})}{T_1T(^6\text{Li})} = \left( \frac{\gamma(^6\text{Li})}{\gamma(^7\text{Li})} \right)^2 \approx 0.14 \quad (2)$$

which is within the range of the experimental value of 0.12 (see SI). Because of the documented deviations<sup>71</sup> between observed and calculated Knight shift  $K$ , we consider it to be a fitting parameter, which here amounts to 80 ppm. We conclude that the  $^6\text{Li}$  and  $^7\text{Li}$  SLR NMR data in the low-temperature regime are consistent with the macroscopic metallic properties of  $\text{Li}_2\text{N}_2$ .

In the temperature-dependent  $T_1$  relaxation rate diagram (see Figure 2), we observe a flat low-temperature regime in

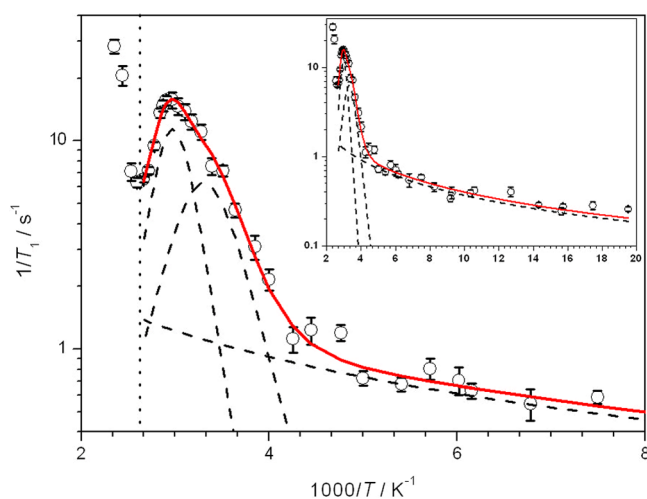


**Figure 2.** Experimental inverse-temperature dependence of the  $^7\text{Li}$  (circles) NMR SLR rates on a logarithmic scale. The fit (solid line) to the experimental data is given by the extended BPP relation (see eq 4). The dashed curves below refer to three different relaxation processes (individual terms in eq 4). The inset shows an overview over the complete data set including the low-temperature region. Decomposition of  $\text{Li}_2\text{N}_2$  is observed at about  $1000/T = 2.6 \text{ K}^{-1}$  (385 K) marked by a dotted line, in good agreement with previous temperature-dependent *in situ* X-ray diffraction analysis.<sup>22</sup>

agreement with metallic relaxation; then, we pass through a maximum at about 300 K which is followed by another rise caused by the decomposition of  $\text{Li}_2\text{N}_2$  to  $\alpha\text{-Li}_3\text{N}$ . The decomposition product  $\alpha\text{-Li}_3\text{N}$  was confirmed by powder X-ray diffraction after the NMR experiments, in line with previous observations.<sup>22</sup>

We interpret the maximum at 300 K as a consequence of Li ion conduction because other explanations such as decomposition to other products because of humidity or temperature can be ruled out on the basis of IR spectroscopy and XRD diffractometry, which show no evidence of decomposition of  $\text{Li}_2\text{N}_2$ .

In the following, we analyze the presented relaxation rates for activation energies and jump rates. In good approximation, the relaxation rates  $1/T_1$  for  $^6,7\text{Li}$  of different relaxation mechanisms add up to the observable relaxation rate  $1/T_1$ :

$$\frac{1}{T_1} = \frac{1}{T_1^{\text{quadrupolar}}} + \frac{1}{T_1^{\text{dipolar}}} + \frac{1}{T_1^{\text{paramagnetic}}} + \dots \quad (3)$$

The most important mechanisms, which are commonly considered for  $^6,7\text{Li}$  NMR of dielectric materials, are relaxation by dipolar, quadrupolar, and paramagnetic mechanisms. The temperature dependence of the first two terms can be estimated from a theory suggested by Bloembergen, Purcell, and Pound (BPP theory).<sup>72</sup> In the low temperature regime, we already realized that an extra term will be necessary, which takes into account the relaxation caused by the random field caused by the conduction electrons. This extra term can be derived from eq 1. For least-squares fitting we neglected the paramagnetic term, we used the following equation which describes quadrupolar/dipolar relaxation through two different terms<sup>73</sup> and added a last term for relaxation through the conduction electrons

$$\begin{aligned} \frac{1}{T_1} = & C_1 \left( \frac{\tau_{c1}}{1 + \omega_0^2 \tau_{c1}^2} + \frac{4\tau_{c1}}{1 + 4\omega_0^2 \tau_{c1}^2} \right) \\ & + C_2 \left( \frac{\tau_{c2}}{1 + \omega_0^2 \tau_{c2}^2} + \frac{4\tau_{c2}}{1 + 4\omega_0^2 \tau_{c2}^2} \right) \\ & + \left( \frac{8\pi^2 T k_B K^2}{h} \frac{\gamma_n^2}{\gamma_e^2} \right) \end{aligned} \quad (4)$$

where  $\tau_{c1}$  and  $\tau_{c2}$  are the correlation times of two motional processes, which can be justified for example by motional heterogeneity.<sup>73</sup> We achieve good agreement (see Figure 2) with the experimental data by assuming that these processes are thermally activated and follow an Arrhenius law  $\tau_c = \tau_0 \exp(E_A/k_B T)$ . Clearly, this is a crude approximation neglecting for example the existence of different crystallographic orbits for Li in the crystal structure of  $\text{Li}_2\text{N}_2$ , biexponential longitudinal relaxation, relaxational anisotropy, correlated motion, and different relaxation rates in the satellite and central transitions.

From least-squares fitting of the  $^7\text{Li}$  NMR SLR experiments, we obtain two different activation energies of 0.57 and 0.34 eV (Table 2), which could reflect the mentioned motional heterogeneity of the Li atoms migrating through the complex structure of  $\text{Li}_2\text{N}_2$ . We note that such a two-component fit yields rather uncommon values  $\tau_0$ . For comparison, a single component fit yields an activation energy  $E_A$  of 0.36 eV, a  $\tau_0$  of  $1.3 \cdot 10^{-15} \text{ s}$ , and a  $C$  of  $13.5 \cdot 10^9 \text{ s}^{-2}$ . A corresponding analysis of SLR rates of  $^6\text{Li}$  NMR measurements (see SI Figure S2) is hampered by the poor signal-to-noise ratio, due to the small

**Table 2. Resulting Refined Parameters of the Analysis of  $^7\text{Li}$  SLR Rates According to Equation 4**

parameter	$i = 1$	$i = 2$
$E_{A,i}/\text{eV}$	0.57	0.34
$C_i/\text{s}^{-2}$	$9.8 \cdot 10^9$	$5.4 \cdot 10^9$
$\tau_{0,i}/\text{s}$	$2.0 \cdot 10^{-18}$	$9.9 \cdot 10^{-16}$

amount of available material, despite isotopic labeling and a handmade sample-container-adapted coil. However, we can use the obtained  $^6\text{Li}$  SLR data set to check whether relaxation is dominated by a quadrupolar or dipolar mechanism. The isotope-dependent factor in the prefactor  $C$  in eq 4 is proportional to  $[I(I + 1)]\gamma^4$  and  $Q^2[(2I+3)/(I^2(2I-1))]$  for a homonuclear dipolar or quadrupolar mechanism,<sup>74–76</sup> respectively, where  $I$  refers to the spin-quantum number,  $Q$  to the quadrupolar moment, and  $\gamma$  to the gyromagnetic ratio, as tabulated by IUPAC.<sup>77</sup> For a dipolar relaxation mechanism neglecting isotope effects the prefactor ratio becomes

$$\frac{C(^6\text{Li})}{C(^7\text{Li})} \approx 0.011 \quad (5)$$

and for quadrupolar relaxation

$$\frac{C(^6\text{Li})}{C(^7\text{Li})} \approx 0.0015 \quad (6)$$

Thus, the SLR of  $^6\text{Li}$  can be predicted on the basis of the  $^7\text{Li}$  least-squares fitting results for the two limiting cases. The resulting comparison with the experimental  $^6\text{Li}$  SLR data (see SI Figure S3) indicates that the dominating mechanism is dipolar in nature.

**Dimensionality of the Motional Process.** Efficient macroscopic Li ion conduction requires three-dimensional (3D) motion of the ions which is further supported by topological analysis of possible lithium migration pathways inside the  $\text{Li}_2\text{N}_2$  structure, as implemented in the software package TOPOS.<sup>78–81</sup> Lithium ions are assumed to be able to jump between different sites if open channels between two sites exist. Formally, a channel is considered accessible for lithium motion if the sum of radii of a lithium ion and a framework atom does not exceed the channel radius more than by 10–15%.<sup>81</sup> The TOPOS software allows to calculate channels and voids with the help of Voronoi-Dirichlet polyhedra. On the basis of such an analysis of the  $\text{Li}_2\text{N}_2$  crystal structure (see Figure 3), it is clear that migration pathways in all three dimensions exist.

Interestingly, only two of the three crystallographic independent Li sites (Li2 and Li3) contribute to possible pathways, whereas Li1 is not free to leave its position (see Figure 3) and thus does not contribute to charge transport. This is due to the fact, that the Li1–N distance of 2.055(1) Å is the shortest of all Li–N distances (2.055–2.180(1) Å), whereby Li1 seems to be trapped at its crystallographic site by  $[\text{N}_2]^{2-}$  ions.<sup>22</sup> Due to the limited resolution power of the static  $^7\text{Li}$  NMR experiments, however, only a single, averaged activation energy can be resolved.

#### Temperature-Dependent Self-Diffusion Coefficients.

In the case of an material with a single Li site, only the inverse correlation time  $\tau_c^{-1}$  corresponds to the  $\text{Li}^+$  jump rate, which allows for an estimate of the self-diffusion coefficient  $D(T)$  of the Li ions according to the Einstein–Smoluchowski relation:<sup>82,83</sup>

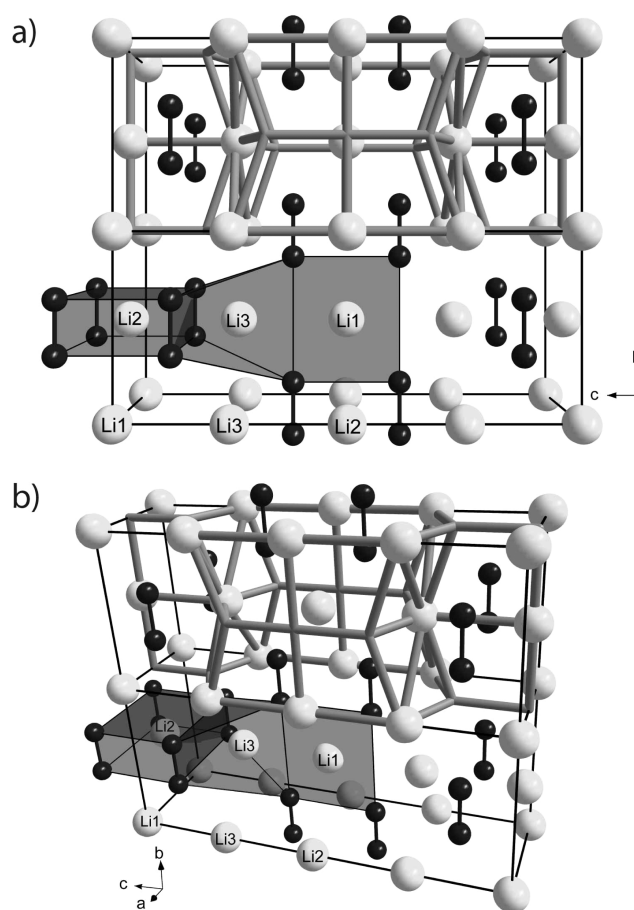


**Figure 3.** [010]-doubled crystal structure of  $\text{Li}_2\text{N}_2$  (Li white, N black) illustrating the calculated possible  $\text{Li}^+$  ion pathways (thick dark gray) according to the voids in the structure obtained by topological analysis. Polyhedra (gray) around Li sites illustrate the coordination spheres of the  $\text{Li}^+$  ions. Cell edges of the unit cells are marked by black lines.

$$D(T) = \frac{l^2}{2d\tau_c} \quad (7)$$

We use this equation to obtain a crude estimate for the self-diffusion of lithium diazenide. To this end, we assume an average jump length  $l$  for the lithium ions between Li sites exists, which contribute to ionic conduction (see SI Figure S4). In addition, each  $\text{Li}^+$  jump is assumed to have the same activation energy, which is actually supposed to vary concerning the topostructural analysis. With  $l = 2.25(1)$  Å and three-dimensional lithium migration ( $d = 3$ ), the calculated self-diffusion coefficients for lithium motion according to the single fit of SLR rates are of the order of  $10^{-14}$  to  $10^{-12}$   $\text{m}^2/\text{s}$  within the corresponding  $\text{Li}^+$  ion conductive temperature range. As-obtained self-diffusion coefficients are approximately within the range of typical cathode and electrolyte materials for Li-ion batteries ( $\text{LiCoO}_2 \sim 10^{-16}$   $\text{m}^2/\text{s}$ ,  $\text{LiBF}_4 \sim 10^{-13}$   $\text{m}^2/\text{s}$ ,  $(\text{Li}_2\text{S})_7(\text{P}_2\text{S}_5)_3 \sim 10^{-12}$   $\text{m}^2/\text{s}$ ).<sup>84–86</sup>

## CONCLUSION

With our experimental study of the unsettled electronic behavior of diazenide compounds, we have shown that alkaline earth diazenides are of true metallic nature. For  $\text{Li}_2\text{N}_2$  the electrical conductivity, unusually, has both electronic and ionic contributions, especially in the high temperature regime. Our

investigations concerning lithium ionic conductivity in  $\text{Li}_2\text{N}_2$  reveal that lithium diazenide is a potential 3D ionic conductor with high Li self-diffusion coefficients. Analysis of spin-lattice relaxation data from  $^6\text{Li}$  and  $^7\text{Li}$  NMR experiments is consistent with contributions from different relaxational mechanisms, namely an electronic contribution describable with the Korringa equation and an ionic contribution of dipolar origin.

## ■ ASSOCIATED CONTENT

### ■ Supporting Information

Infrared spectra (Figure S1) of  $^{6,7}\text{Li}_2\text{N}_2$  and  $M_{\text{AE}}\text{N}_2$  ( $M_{\text{AE}} = \text{Ca}, \text{Sr}, \text{Ba}$ ), plot of  $1/(T_1T)$  versus temperature for  $^6\text{Li}$  and  $^7\text{Li}$  NMR SLR rates (Figure S2),  $^6\text{Li}$  NMR SLR rates versus temperature (Figure S3), analysis of line width and chemical shift of the  $^6\text{Li}$  NMR signal in  $^6\text{Li}_2\text{N}_2$  (see Figure S4), as well as details of the calculation of the average jump length  $l$  of the lithium motion for the crude estimate of the self-diffusion coefficients  $D(T)$  (Figure S5 and Table S1). This material is available free of charge via the Internet at <http://pubs.acs.org>.

## ■ AUTHOR INFORMATION

### Corresponding Author

\*Fax: +49089-2180-77440. Tel: +49089-2180-77436. E-mail: wolfgang.schnick@uni-muenchen.de.

### Notes

The authors declare no competing financial interest.

## ■ ACKNOWLEDGMENTS

The authors thank Prof. Dirk Johrendt (LMU Munich) for providing the equipment for the conductivity measurements, as well as Dr. Thomas Bräuniger and Christian Minke for technical support with the NMR spectrometer (both LMU Munich). Furthermore, the authors gratefully acknowledge financial support from the Fonds der Chemischen Industrie (FCI) and the Deutsche Forschungsgemeinschaft (DFG), project SCHN 377/13-2.

## ■ REFERENCES

- (1) Matoba, G. Patent No. JP-B 50010804, 1975; Matoba, G. Patent JP-B 50010803, 1975; Kobayashi, H. Patent No. JP-A 03006314, 1991; Chokei, T. Patent No. JP 55094432, 1980; Willners, H. Patent No. SE 115621, 1946.
- (2) Jhi, S. H.; Ihm, J.; Louie, S. G.; Cohen, M. L. *Nature* **1999**, *399*, 132.
- (3) McMillan, P. F. *Nat. Mater.* **2002**, *1*, 19.
- (4) Maruyama, T.; Morishita, T. *Appl. Phys. Lett.* **1996**, *69*, 890.
- (5) Yamanaka, S.; Hotehama, K.; Kawaji, H. *Nature* **1998**, *392*, 580.
- (6) Zerr, A.; Miehe, G.; Boehler, R. *Nat. Mater.* **2003**, *2*, 185.
- (7) Chhowalla, M.; Unalan, H. E. *Nat. Mater.* **2005**, *4*, 317.
- (8) Leineweber, A.; Jacobs, H.; Hull, S. *Inorg. Chem.* **2001**, *40*, 5818.
- (9) Wu, Z. G.; Chen, X. J.; Struzhkin, V. V.; Cohen, R. E. *Phys. Rev. B* **2005**, *71*, 214103.
- (10) Pfirrmann, S.; Herwig, C.; Stöber, R.; Ziemer, B.; Limberg, C. *Angew. Chem.* **2009**, *121*, 3407–3411; *Angew. Chem., Int. Ed.* **2009**, *48*, 3357.
- (11) Chirik, P. J. *Nature Chem.* **2009**, *1*, 520.
- (12) Evans, W. J.; Fang, M.; Zucchi, G.; Furche, F.; Ziller, J. W.; Hoekstra, R. M.; Zink, J. I. *J. Am. Chem. Soc.* **2009**, *131*, 11195.
- (13) Kaim, W.; Sarkar, B. *Angew. Chem.* **2009**, *121*, 9573; *Angew. Chem., Int. Ed.* **2009**, *48*, 9409.
- (14) Uhl, W.; Rezaeirad, B.; Layh, M.; Hagemeyer, E.; Würthwein, E.-U.; Ghavtadze, N.; Kuzu, I. *Chem.—Eur. J.* **2010**, *16*, 12195.
- (15) Rinehart, J. D.; Fang, M.; Evans, W. J.; Long, J. R. *Nat. Chem.* **2011**, *3*, 538.

- (16) Farnaby, J. H.; Fang, M.; Ziller, J. W.; Evans, W. J. *Inorg. Chem.* **2012**, *51*, 11168.
- (17) Auffermann, G.; Prots, Y.; Kniep, R. *Angew. Chem.* **2001**, *113*, 565; *Angew. Chem., Int. Ed.* **2001**, *40*, 547.
- (18) Vajenine, G. V.; Auffermann, G.; Prots, Y.; Schelle, W.; Kremer, R. K.; Simon, A.; Kniep, R. *Inorg. Chem.* **2001**, *40*, 4866.
- (19) Auffermann, G.; Schmidt, U.; Bayer, B.; Prots, Y.; Kniep, R. *Anal. Bioanal. Chem.* **2002**, *373*, 880.
- (20) Auffermann, G.; Kniep, R.; Bronger, W. Z. *Anorg. Allg. Chem.* **2006**, *632*, 565.
- (21) Prots, Y.; Auffermann, G.; Tovar, M.; Kniep, R. *Angew. Chem.* **2002**, *114*, 2392; *Angew. Chem., Int. Ed.* **2002**, *41*, 2288.
- (22) Schneider, S. B.; Frankovsky, R.; Schnick, W. *Angew. Chem.* **2012**, *124*, 1909; *Angew. Chem., Int. Ed.* **2012**, *51*, 1873.
- (23) S. Schneider, S. B.; Frankovsky, R.; Schnick, W. *Inorg. Chem.* **2012**, *51*, 2366.
- (24) Gregoryanz, E.; Sanloup, C.; Somayazulu, M.; Badro, J.; Fiquet, G.; Mao, H.-K.; Hemely, R. J. *Nat. Mater.* **2004**, *3*, 294.
- (25) von Appen, J.; Lumey, M.-W.; Dronskowski, R. *Angew. Chem.* **2006**, *118*, 4472; *Angew. Chem., Int. Ed.* **2006**, *45*, 4365.
- (26) Crowhurst, J. C.; Goncharov, A. F.; Sadigh, B.; Evans, C. L.; Morrall, P. G.; Ferreira, J. L.; Nelson, A. J. *Science* **2006**, *311*, 1275.
- (27) Young, A. F.; Montoya, J. A.; Sanloup, C.; Lazzeri, M.; Gregoryanz, E.; Scandolo, S. *Phys. Rev. B* **2006**, *73*, 153102.
- (28) Montoya, J. A.; Hernandez, A. D.; Sanloup, C.; Gregoryanz, E.; Scandolo, S. *Appl. Phys. Lett.* **2007**, *90*, 011909.
- (29) Crowhurst, J. C.; Goncharov, A. F.; Sadigh, B.; Zaug, J. M.; Aberg, D.; Meng, Y.; Prakapenka, V. B. *J. Mater. Res.* **2008**, *23*, 1.
- (30) Chen, Z. W.; Guo, X. J.; Liu, Z. Y.; Ma, M. Z.; Jing, Q.; Li, G.; Zhang, X. Y.; Li, L. X.; Wang, Q.; Tian, Y. J.; Liu, R. P. *Phys. Rev. B* **2007**, *75*, 054103.
- (31) Yu, R.; Zhan, Q.; De Jonghe, L. C. *Angew. Chem.* **2007**, *119*, 1154; *Angew. Chem., Int. Ed.* **2007**, *46*, 1136.
- (32) Chen, W.; Tse, J. S.; Jiang, J. Z. *J. Phys.: Condens. Matter* **2010**, *22*, 015404.
- (33) Wessel, M.; Dronskowski, R. *J. Am. Chem. Soc.* **2010**, *132*, 2421.
- (34) Wessel, M.; Dronskowski, R. *J. Comput. Chem.* **2010**, *31*, 1613.
- (35) Ruschewitz, U. *Coord. Chem. Rev.* **2003**, *244*, 115.
- (36) Kockelmann, W.; Ruschewitz, U. *Angew. Chem.* **1999**, *111*, 3697; *Angew. Chem., Int. Ed.* **1999**, *38*, 3492.
- (37) Hemmersbach, S.; Zibrowius, B.; Kockelmann, W.; Ruschewitz, U. *Chem.—Eur. J.* **2001**, *7*, 1952.
- (38) Weidlein, J.; Müller, U.; Dehnicke, K. *Schwingungsspektroskopie—Eine Einführung*; Georg Thieme Verlag: Stuttgart, NY, 1982.
- (39) Wessel, M.; Dronskowski, R. *Chem.—Eur. J.* **2011**, *17*, 2598.
- (40) Wessel, M. *PhD thesis*, RWTH Aachen University, Aachen, 2010.
- (41) Knauth, P. *Solid State Ionics* **2009**, *180*, 911.
- (42) Park, M.; Zhang, X.; Chung, M.; Less, G. B.; Sastry, A. M. *J. Power Sources* **2010**, *195*, 7904.
- (43) Oudenhoven, J. F. M.; Baggetto, L.; Notten, P. H. L. *Adv. Energy Mater.* **2011**, *1*, 10.
- (44) Heitjans, P.; Indris, S. *J. Phys.: Condens. Matter* **2003**, *15*, R1257.
- (45) Grey, C. P.; Dupré, N. *Chem. Rev.* **2004**, *104*, 4493.
- (46) Böhmer, R.; Jeffrey, K. R.; Vogel, M. *Prog. Nucl. Mag. Res. Sp.* **2007**, *50*, 87.
- (47) Boukamp, B. A.; Huggins, R. A. *Phys. Lett.* **1976**, *58A*, 231.
- (48) v. Alpen, U.; Rabenau, A.; Talat, G. H. *Appl. Phys. Lett.* **1977**, *30*, 621.
- (49) Wang, Z.; Gobet, M.; Sarou-Kanian, V.; Massiot, D.; Bessada, C.; Deschamps, M. *Phys. Chem. Chem. Phys.* **2012**, *14*, 13535.
- (50) Mali, M.; Roos, J.; Sonderegger, M.; Brinkmann, D.; Heitjans, P. *J. Phys. F: Met. Phys.* **1988**, *18*, 403.
- (51) Kuhn, A.; Narayanan, S.; Spencer, L.; Goward, G.; Thangadurai, V.; Wilkening, M. *Phys. Rev. B* **2011**, *83*, 094302.
- (52) Kuhn, A.; Sreeraj, P.; Pöttgen, R.; Wiemhöfer, H.-D.; Wilkening, M.; Heitjans, P. *J. Am. Chem. Soc.* **2011**, *133*, 11018.
- (53) Koch, B.; Vogel, M. *Solid State Nucl. Magn. Reson.* **2008**, *34*, 37.

- (54) Ehrlich, P.; Seifert, H. J.; Brauer, G. *Handbuch der Präparativen Anorganischen Chemie Vol. 2*; Ferdinand Enke Verlag: Stuttgart, 1978.
- (55) Remy-Gennete, P. *Ann. Chim.* **1933**, *19*, 289.
- (56) Fair, H. D.; Walker, R. F. *Energetic Materials Vol. 1: Physics and Chemistry of the Inorganic Azides*, Plenum Press: New York, 1977.
- (57) Walker, D.; Carpenter, M. A.; Hitch, C. M. *Am. Mineral.* **1990**, *75*, 1020.
- (58) Walker, D. *Am. Mineral.* **1991**, *76*, 1092.
- (59) Huppertz, H. Z. *Kristallogr.* **2004**, *219*, 330.
- (60) Rubie, D. C. *Phase Transitions* **1999**, *68*, 431.
- (61) Kawai, N.; Endo, S. *Rev. Sci. Instrum.* **1970**, *8*, 1178.
- (62) van-der-Pauw, L. J. *Philips Research Reports* **1958**, *13*, 1.
- (63) Powles, J. G.; Strange, H. *Proc. Phys. Soc* **1963**, *6*, 82.
- (64) The actual measurements have been performed with non-sintered pellets due to the observation that upon sintering using different conditions (temperatures, crucibles, atmospheres) always the beginning of hydrolysis of the pellets (white surrounding) was detected. Thus, the white hydroxide layer inhibits the contact of the inner-sphere diazenide to the electrodes making conductivity measurements impossible.
- (65) Weast, R. C. *Handbook of Chemistry and Physics*; CRC Press: Cleveland, OH, 1975.
- (66) Kaye, G. W. C.; Laby, T. H. *Tables of physical and Chemical Constants*, 15<sup>th</sup> ed.; Longman: London, 1993.
- (67) Upon variable temperature NMR measurements, the decomposition temperature of  ${}^7\text{Li}_2\text{N}_2$  is found to be approximately 385 K due to a further sharp increase in inverse  $T_1$  data. However, a corresponding NMR analysis of  ${}^6\text{Li}_2\text{N}_2$  yields a decomposition temperature about 40 K lower. On the one hand, the divergence in decomposition temperature is referred to the limited data quality of  ${}^6\text{Li}$  measurements, hindering a proper identification of the phase transition from  $\text{Li}_2\text{N}_2$  to  $\text{Li}_3\text{N}$ . On the other hand, the synthesis of  ${}^6\text{Li}_2\text{N}_2$  includes many more steps as compared to  ${}^7\text{Li}_2\text{N}_2$  synthesis, whereby the final product  ${}^6\text{Li}_2\text{N}_2$  might be afflicted with more side phases possibly changing the true decomposition temperature of  ${}^6\text{Li}_2\text{N}_2$ .
- (68) van der Klink, J. J.; Brom, H. B. *Prog. Nuclear Magn. Reson. Spectrosc.* **2000**, *36*, 89.
- (69) Korryng, J. *Physica* **1950**, *16*, 601.
- (70) Avadhut, Y. S.; Weber, J.; Hammarberg, E.; Feldmann, C.; Schmedt auf der Günne, J. *Phys. Chem. Chem. Phys.* **2012**, *14*, 11610.
- (71) Slichter, C. P. *Principles of Magnetic Resonance*; Springer-Verlag: Berlin, 1992.
- (72) Bloembergen, N.; Purcell, E. M.; Pound, R. V. *Phys. Rev.* **1948**, *73*, 679.
- (73) Arbi, K.; París, M. A.; Sanz, J. *Dalton Trans.* **2011**, *40*, 10195.
- (74) Solomon, I. *Phys. Rev.* **1955**, *99*, 559.
- (75) León, C.; Lucìa, M. L.; Santamarià, J.; París, M. A.; Sanz, J.; Várez, A. *Phys. Rev. B* **1996**, *54*, 184.
- (76) Sudmeier, J. L.; Anderson, S. E.; Frye, J. S. *Concepts Magn. Reson.* **1990**, *2*, 197.
- (77) Harris, R. K.; Becker, E. D.; Cabral de Menezes, S. M.; Goodfellow, R.; Granger, P. *Solid State Nucl. Mag.* **2002**, *22*, 458.
- (78) Blatov, V. A. *IUCr Comp. Comm. Newsletter* **2006**, *7*, 4.
- (79) Blatov, V. A. *Acta Crystallogr., Sect. A: Cryst. Found. Crystallogr.* **2000**, *56*, 178.
- (80) Blatov, V. A.; Shevchenko, A. P.; Serezhkin, V. N. *J. Appl. Crystallogr.* **1999**, *32*, 377.
- (81) Blatov, V. A.; Ilyushin, G. D.; Blatova, O. A.; Anurova, N. A.; Ivanov-Schits, A. K.; Dem'yanets, L. N. *Acta Crystallogr.* **2006**, *B62*, 1010.
- (82) Einstein, A. *Ann. Phys.* **1905**, *17*, 549.
- (83) von Smoluchowski, M. *Ann. Phys.* **1906**, *21*, 756.
- (84) Jang, Y. I.; Neudecker, B. J.; Dudney, N. J. *Electrochem. Solid-State Lett.* **2001**, *4*, A74.
- (85) Wu, T.-Y.; Hao, L.; Kuo, C.-W.; Lin, Y.-C.; Su, S.-G.; Kuo, P.-L.; Sun, I.-W. *Int. J. Electrochem. Sci.* **2012**, *7*, 2047.
- (86) Hayamizu, K.; Aihara, Y. *Solid State Ionics* **2013**, *238*, 7.